ELSEVIER

Thermochimica Acta 348 (2000) 77–89

thermochimica acta

www.elsevier.com/locate/tca

Quantitative analysis of errors in TMDSC in the glass transition region

Sindee L. Simon*, Gregory B. McKenna

Department of Chemical Engineering, Texas Tech University, Lubbock, TX 79409, USA

Received 10 June 1999; received in revised form 24 November 1999; accepted 29 November 1999

Abstract

Temperature modulated differential scanning calorimetry (TMDSC) data are simulated through the glass transition region using the Tool–Narayanaswamy–Moynihan (TNM) model of structural recovery. The simulated data are analyzed using a fast Fourier transform similar to conventional Temperature-modulated differential scanning calorimetry techniques. The glass transition temperature (T_g) and enthalpy of aging (ΔH_a) were calculated from the simulated data and compared with the values expected based on linear isothermal simulations for the case of the glass temperature and based on the input simulated data for ΔH_a. The errors associated with the TMDSC data analysis were thus quantified.

Keywords: Calorimetry; Scanning calorimetry; Temperature-modulated differential scanning calorimetry; Dynamic calorimetry; Structural recovery; Tool–Narayanaswamy model

1. Introduction

Temperature-modulated differential scanning calorimetry (TMDSC) is a new thermal analysis technique in which the normal temperature scan used in DSC is overlaid generally by a sinusoidal temperature perturbation having a frequency ranging from approximately 0.01 to 0.1 Hz [1]. The sinusoidal heat flow required to maintain the desired sinusoidal temperature history is the quantity measured in the TMDSC experiment. The purported advantages of TMDSC include improved resolution and sensitivity and the ability to separate overlapping phenomena [2]. The focus of this work is on the use of TMDSC to separate the endothermic step change observed at the glass temperature from the endothermic excess enthalpy annealing peak observed in aged glasses.

Before we discuss the assumptions behind the TMDSC data analysis, we review the glass transition and the enthlapy (H) vs. temperature (T) behavior shown in Fig. 1a. At high temperatures the material is at equilibrium. During cooling from equilibrium, the molecular mobility of the material decreases, and at the glass temperature (T_g), the material is no longer able to maintain equilibrium in the timescale of cooling and the enthlapy departs from the equilibrium line and moves onto the glass line. The solid curve shows this behavior schematically. It is important to understand that this departure from the equilibrium line depends on the rate of cooling. A faster cooling rate results in departure from equilibrium at a higher temperature. This also means that T_g is frequency

* Corresponding author. Tel.: +1-806-780-1763; fax: +1-806-742-3552.
E-mail address: sindee.simon@coe.ttu.edu (S.L. Simon)

0040-6031/00/$ – see front matter
PII: S0040-6031(99)00482-7

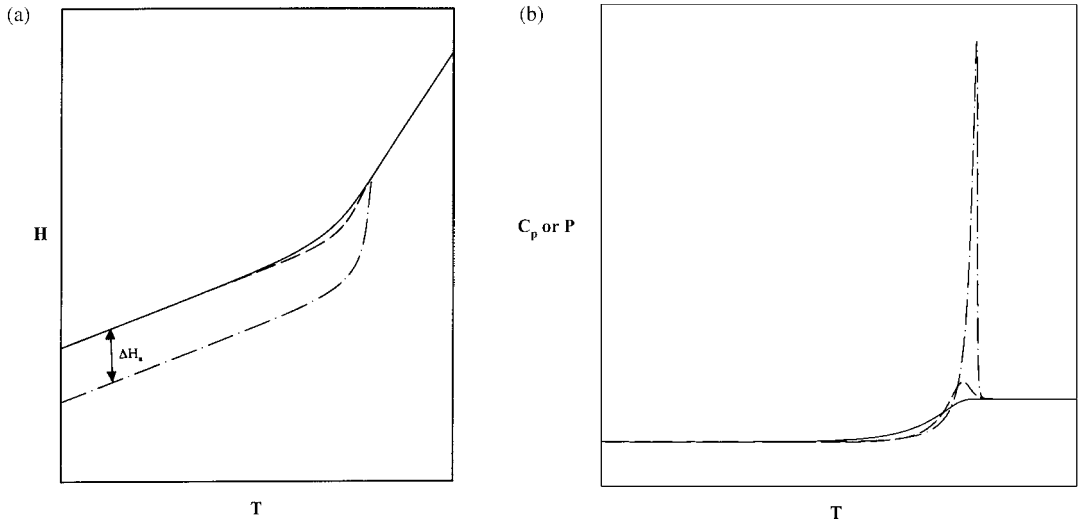

Fig. 1. (a) Schematic representation of enthalpy vs. temperature for cooling, heating, and aging treatments. Solid line represents the response on cooling at a rate q. Dashed line represents response on heating at a rate q immediately after cooling. Dashed-dot line represents the response on heating of an aged glass. (b) Schematic representation of the heat capacity or the heat flow vs. temperature for cooling, heating, and aging treatments. Solid line represents the response on cooling at a rate q. Dashed line represents the response on heating at a rate q immediately after cooling. Dashed-dot line represents the response on heating of an aged glass. Note the large excess enthalpy peak for the aged curve and the shifting of the apparent position of the glass transition.

dependent and, thus, is expected to depend on the modulation period in TMDSC.

Still referring to Fig. 1a, we now look at what happens to the enthalpy during heating (without modulation). For an unaged glass, i.e., if no relaxation occurs isothermally in the glassy state or during heating, the dashed curve is observed during heating. Some small hysteresis in the vicinity of T_g is observed between the cooling and heating scans. On the other hand, the dashed-dot line shows the behavior on heating of an aged glass. Since the aged glass has lower molecular mobility (corresponding to its increased density), the enthalpy often overshoots the equilibrium line during heating such that the rapid increase to equilibrium occurs at a temperature considerably above the glass temperature as shown. The corresponding heat flow (P) or apparent heat capacity (C_p) for the aged and unaged glasses is shown in Fig. 1b. For the unaged material, there is simply an endothermic step change in the heat flow at T_g. For the aged glass, an annealing peak is observed. The difference between the area under the ideal curve and that of the aged glass is the difference in enthalpy between the glass lines for the unaged and aged glasses (ΔH_a) [3]. In traditional DSC, ΔH_a is obtained by performing a temperature scan for an aged glass to obtain the aged response, then quenching the material at a given rate, and performing a second temperature scan without aging the material to obtain the unaged response. A purported advantage of TMDSC is the ability to obtain the same information with only one temperature scan.

In commercial instruments, the results of the TMDSC experiment are reported in terms of reversing and non-reversing heat flows [1,4]. The reversing component is obtained from the amplitude of the first harmonic of the heat flow using a Fourier transform of the data (or an approximation thereof), and the non-reversing heat flow is the difference between the average heat flow and the reversing heat flow. In what follows we show that the average heat flow approximates the heat flow from a conventional DSC experiment when the modulation does not cause significant distortions. In the standard TMDSC analysis, it is assumed that the reversing heat flow is due to changes in the sensible heat ($C_p\ \mathrm{d}T$ term) and that all kinetic events are reflected in the non-reversing heat flow. If this were the case, then the reversing heat flow would show an endothermic step change at the glass transition, and the non-reversing heat flow would give a

peak whose area would be the enthalpy difference between the aged and unaged glasses (ΔH_a in Fig. 1). The assumption implies not only that the step change at the glass transition contributes only to the first harmonic in the heat flow and that the structural recovery leading to the annealing peak does not, but also that the kinetics associated with structural recovery near the glass transition are a linear process, which they are not.

A second important issue is the interaction between the heating rate and the measurement frequency. This effect has been reported by various researchers, including the commercial TMDSC manufacturers. The latter suggested that at least four cycles need to be present during the transition of interest in order to get meaningful reversing and non-reversing heat flows [1]. More recently, Snyder and Mopsik [5] have shown that the results of dynamic measurements made during a temperature ramp can be dubious, particularly for the combination of a low frequency probe with a high scanning rate because an anomalous dynamically induced loss will be present.

We note that a dynamic heat capacity data analysis technique has been suggested by Schawe [6] yielding a storage heat capacity (C_p') and a loss heat capacity (C_p''). The approach is similar to that used in the dynamic heat spectroscopy measurements pioneered by Birge and Nagel [7,8]. However, as Schawe notes, this approach is valid only if the response is linear, and we have shown that the TMDSC response is non-linear for structural relaxation at the glass transition due to the kinetics of the processes coupled with the ramping temperature [3]. Furthermore, because of this non-linearity, the phase angle obtained in a linear analysis is not expected to give meaningful information concerning the aged glass. In fact, Hutchinson and Montserrat [9] have recently shown, using simulated data from a model using one relaxation time, that C_p'' was small and unrelated to the enthalpic state of the glass, i.e., ΔH_a.

In a previous work, we used the Tool–Narayanaswamy–Moynihan (TNM) model [10,11,13] to simulate TMDSC data through the glass transition region [12]. A qualitative Lissajous loop analysis showed that the data was not linear through the glass transition, and that the degree of non-linearity increased as the magnitude of the excess enthalpy annealing peak increased. In this work, we use fast Fourier transforms to perform a quantitative analysis of the simulated TMDSC data for glasses obtained with various thermal histories and modulation frequencies. Our results show that the above-described TMDSC data analysis method provides estimates for the glass transition temperature within 1–2°C of the correct value. At the same time, the equivalence made between the non-reversing heat flow (ΔH_{non}) and ΔH_a can lead to substantial errors.

We divide our simulated experiments into three cases. The first case is one in which there are enthalpy overshoots, as shown schematically by the dashed-lines in Fig. 1a and b; such behavior is observed when the cooling rate is considerably less than the heating rate. The second case is for enthalpy undershoots. An enthalpy undershoot is observed when the cooling rate is considerably greater than the heating rate and relaxation occurs during heating; such behavior is shown schematically in Fig. 2a and b for enthalpy and heat flow, respectively. The third situation deals with the interaction of the modulation period and the heating rate rather than specifically with the thermal history of the glass; in particular, we examine the response when the heating rate is such that there are relatively few cycles through the transition region. In all cases, we compare the glass transition temperature determined from the reversing heat flow to that expected based on linear simulations. We also compare the values of ΔH_a determined from the non-reversing heat flows to the values expected from the simulated data. In this way we are able to quantify the errors in the analysis methodology.

The paper is organized as follows. We review the TNM model of structural recovery and its application to simulate the TMDSC experiment. We then discuss how the Fourier analysis is used to obtain information relevant to the reversing and non-reversing heat flows. Subsequently we present and discuss the results. We end with a brief conclusion.

2. Modeling TMDSC response in glass-forming materials

2.1. Material response equations

The output of TMDSC is heat flow as a function of time and/or temperature. We calculate the heat flow by

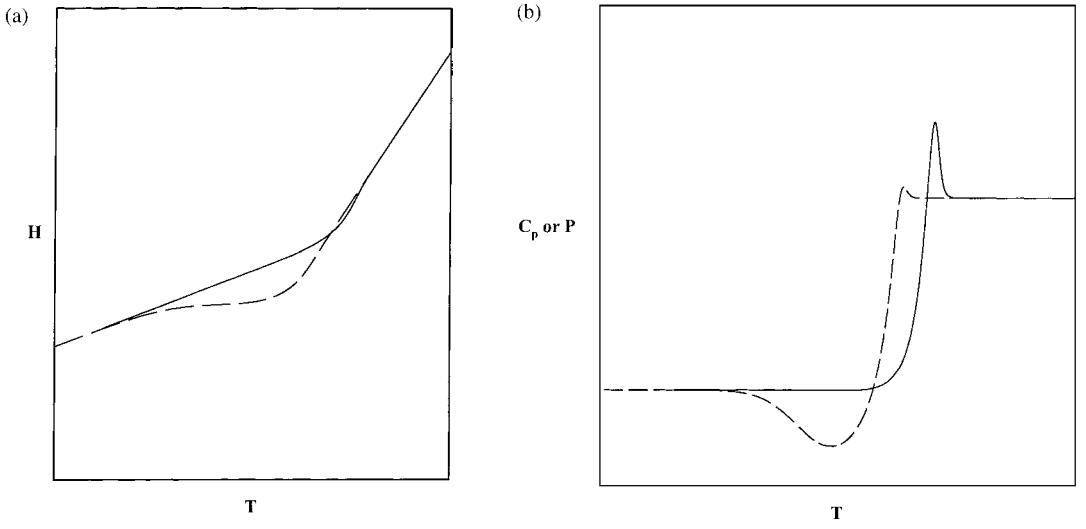

Fig. 2. (a) Schematic representation of enthalpy vs. temperature for DSC heating scans after cooling at a high rate for heating at the same rate (solid line). The dashed line represents the response during heating after cooling at a much slower rate. (b) Schematic representation of heat capacity or the heat flow vs. temperature during DSC heating scans for different conditions. The solid line is for heating at a rate q after cooling at the same rate. The dashed line is for heating at a rate which is much slower than the cooling rate. (Note the undershoot in the DSC trace when the heating rate is much slower than the cooling rate.)

noting that it is the time derivative of the enthalpy, which is in turn a function only of temperature in the equilibrium state (at constant pressure). In the glassy state, however, enthalpy is dependent on the temperature and on the structure of the glass. A convenient measure of the structure of the glass is the fictive temperature, T_f, originally defined by Tool [13]. (T_f is defined as the temperature at which the enthalpy extrapolated along the glassy line would equal the equilibrium value as shown in Fig. 1 for the aged glass.) Assuming that the enthalpy of the equilibrium liquid at 0 K is zero and the heat capacity in the liquid and glass are independent of temperature, the enthalpy (H) of an amorphous material can be written as follows:

$$H = \Delta C_p(T_f - T) + C_{pl}T = \Delta C_p T_f + C_{pg}T \quad (1)$$

where ΔC_p is the difference in heat capacity between the equilibrium (liquid) and glassy states: $\Delta C_p = C_{pl} - C_{pg}$, where C_{pl} and C_{pg} are the heat capacities of the liquid and glass, respectively. The heat flow (P) is simply the time derivative of the enthalpy:

$$P = \frac{dH}{dt} = \Delta C_p \frac{dT_f}{dt} + C_{pg}\frac{dT}{dt} \quad (2)$$

This equation is equivalent to that derived by Hutchinson and Montserrat [9].

For an ideal experiment in which there is no thermal lag in the sample and no thermal resistance between the sample and the furnace, the instantaneous heating rate in the sample (dT/dt) is equal to that of the program temperature. For this case, the problem of modeling the heat flow during a DSC temperature ramp is one of modeling the structural evolution of the material, i.e., $dT_f/dt = (dT_f/dT)(dT/dt)$. It is noted that in a real TMDSC experiment, there is thermal lag in the sample and that this contributes to the phase lag measured; we have addressed this problem in our previous work [2] but do not address it here.

The Tool–Narayanaswamy–Moynihan model [10,11,13] accounts for the non-linear behavior of glassy materials by including terms for the dependence of molecular mobility on the structure of the glass and for the non-exponential nature of structural (in this case enthalpy) recovery. This model is successful not only in predicting quantitatively the material response to complex thermal histories, but also in providing a physical picture of the reasons for the behavior. A full description of the TNM formulation is given elsewhere [11] and reviews have been written [14–18]; only a brief description follows. According

to the TNM model, the structural recovery process is represented by the generalized Kohlrausch [19]–William–Watts [20] (KWW) function

$$\frac{dT_f}{dT} = 1 - \exp\left\{-\left[\int_0^t (dt/\tau_0)\right]^{\beta}\right\} \quad (3)$$

The non-exponentiality of the recovery process is described by β; the non-linearity is incorporated into the model by allowing the retardation time τ_0 to be a function not only of temperature but also of structure (T_f) (and hence a function of time). Eq. (3) can be solved numerically for the fictive temperature. To model the sinusoidal temperature history in TMDSC, we found that temperature steps of 0.05 K or less gave convergent results in all cases examined [12]. The results presented here meet this criterion.

A phenomenological equation relating the retardation time τ_0 to temperature and structure (T_f) is needed to perform the model calculations. The Tool–Narayanaswamy [10,13] equation is an Arrhenius-like equation and can be used as a good approximation when a small temperature range is considered

$$\ln \tau_0 = \ln A + \frac{x\Delta h}{RT} + \frac{(1-x)\Delta h}{RT_f} \quad (4)$$

The parameter x, introduced by Moynihan et al. [11], partitions the material dependences between temperature and structure (T_f), and Δh and $\ln A$ are assumed to be constants.

2.2. Simulated TMDSC experiment

The evolution of the fictive temperature during a given thermal history is given by the solution of Eq. (4) coupled with an appropriate expression for the relaxation time. The thermal history used for modeling a TMDSC experiment includes the cooling leg from above T_g to a point below T_g and the subsequent heating leg to above T_g. The sinusoidal temperature modulation is generally applied only in the heating leg. We assume an experiment in which no thermal lag is present; therefore, the temperature of the sample is equal to the temperature of the furnace. The thermal history is then

$$T = T_0 - qt, \quad t \le t_1 \quad (5)$$

$$T = T_0 - qt_1 + m(t - t_1) + A\sin[\omega(t - t_1)], \quad t > t_1 \quad (6)$$

where t_1 is the time at which the cooling leg is completed, q the cooling rate, m the heating rate, A the amplitude of the temperature modulation and ω is the radian frequency of the modulation. For the heating leg, the instantaneous heating rate, which is used in Eq. (2) to compute the heat flow, is given by

$$\frac{dT}{dt} = m + A\omega\cos[\omega(t - t_1)], \quad t > t_1 \quad (7)$$

3. Description of simulated experiments and data analysis

Here we used model parameters for polystyrene in our calculations, and these are reported in Table 1. The values were taken from the literature [12,21,22] with the exception of the heat capacity data for polystyrene which was obtained in one of our laboratories [23].

The calculations were performed for cooling rates ranging from 0.01 to 30.0°C/min and for heating rates of 1.0, 2.0, and 5.0°C/min. The modulation amplitude during heating was 1.0°C in all cases. The modulation period (=$2\pi/\omega$) varied from 16 to 256 s. 64 data points were recorded per cycle. For comparison purposes, calculations were also performed to simulate DSC results using the same cooling and heating rates but without modulation.

The fast Fourier transforms [24] were performed on the TMDSC simulated data over one modulation cycle (64 points) for the sinusoidal temperature, sinusoidal

Table 1
Parameters used in model calculations

Material	Polystyrene
T_g (K)	373.2[a]
$\Delta h/R$ (K)	80000[b]
x	0.46[b]
β	0.71[b]
$\ln(A/s)$	−216[b]
C_{pg} (J/g K) at T_g	1.52[c]
C_{pl} (J/g K) at T_g	1.77[c]

[a] From [21].
[b] From [14].
[c] From [23].

heat flow, and sinusoidal heating rate. We performed sliding transforms, and hence a transform is made for every point. The average temperature was obtained from the DC component of the temperature and the average (or total) heat capacity was obtained from the DC value (or average) of the heat flow $\langle P \rangle$ divided by the average or underlying heating rate m:

$$C_{p,\mathrm{ave}} = \frac{\langle P \rangle}{m} \tag{8}$$

The reversing heat capacity was obtained from the first harmonics of the heat flow and heating rate, A_p and $A_{\dot{T}}$, respectively:

$$C_{p,\mathrm{rev}} = \frac{A_p}{A_{\dot{T}}} = \frac{A_p}{\omega A} \tag{9}$$

where A is still the amplitude of the temperature perturbation. The non-reversing heat capacity is the difference between the two:

$$C_{p,\mathrm{non}} = C_{p,\mathrm{ave}} - C_{p,\mathrm{rev}} \tag{10}$$

The midpoint in the step change of the reversing heat flow is defined by us as $T_{\mathrm{g,rev}}$. This TMDSC value of the glass transition temperature as a function of the modulation period is compared with the value of T_g obtained from isothermal linear calculations which are described below. We also examine the change in heat capacity at T_g, ΔC_p, for both the total heat flow and from the reversing heat flow. We are interested both in the value of ΔC_p and in the apparent temperature dependence which arises when $C_{p\mathrm{l}}$ and $C_{p\mathrm{g}}$ do not have or appear to have the same temperature dependence.

From the non-reversing heat flow, we calculated the area of the peak in the non-reversing heat flow, ΔH_{non}, using a sloping baseline (line drawn between the temperatures at the beginning and end of the peak). This enthalpy change is compared to that expected, ΔH_a, based on the value of the fictive temperature of the glass after cooling, T_{fo}:

$$\Delta H_\mathrm{a} = \Delta C_p (T_\mathrm{g} - T_{\mathrm{fo}}) \tag{11}$$

The value of T_g in Eq. (11) is taken to be the linear or theoretical value and the value of ΔC_p is that used to perform the calculations.

As alluded to above, we also carried out isothermal linear calculations at temperatures ranging from 91 to 102°C using modulation amplitudes of 0.1°C and periods ranging from 0.1 to 800 s to determine the theoretical dependence of the glass temperature on the modulation period. Because of the small modulation amplitude, in such calculations $T_\mathrm{f} \approx T$ and Eq. (4) becomes

$$\ln \tau_0 = \ln A + \frac{\Delta h}{RT} \tag{12}$$

This results in a linear response and the calculations are the same as those used to simulate dynamic heat spectroscopy data and are similarly analyzed in terms of a storage and a loss heat capacity, C_p' and C_p'' [25]:

$$C_p' = C_p \cos\delta \tag{13}$$

$$C_p'' = C_p \sin\delta \tag{14}$$

where δ is the phase lag between the heat flow P and the rate of temperature change $\mathrm{d}T/\mathrm{d}t$.

4. Results

We first discuss the results of the linear isothermal calculations since these are compared to the TMDSC results. Fig. 3 shows C_p' and C_p'' vs. the logarithm of the modulation period for temperatures of 91, 93, and 95°C. At a given temperature, C_p' increases from the value of the glass heat capacity at short periods to the value of the liquid heat capacity at long periods. Correspondingly, C_p'' goes through a maximum. The glass transition at a given temperature is defined to occur at the modulation period (frequency) where the maximum in the loss heat capacity occurs. As expected based on Eq. (4), there is a linear relationship between the glass temperature and the logarithm of the modulation period:

$$\ln(\mathrm{period}) = \ln(\mathrm{period})_{T_{\mathrm{g,ref}}} + \frac{\Delta h}{R}\left(\frac{1}{T_{\mathrm{g,ref}}} - \frac{1}{T_\mathrm{g}}\right) \tag{15}$$

This relationship will be shown in graphical form later where it is compared to the T_g obtained from TMDSC simulations. First we describe the TMDSC results in a more qualitative way.

Fig. 4 shows the results for the simulated TMDSC response of polystyrene to an underlying heating rate of 1°C/min after being cooled at 0.1°C/min. The modulation period was 64 s. The reversing, non-rever-

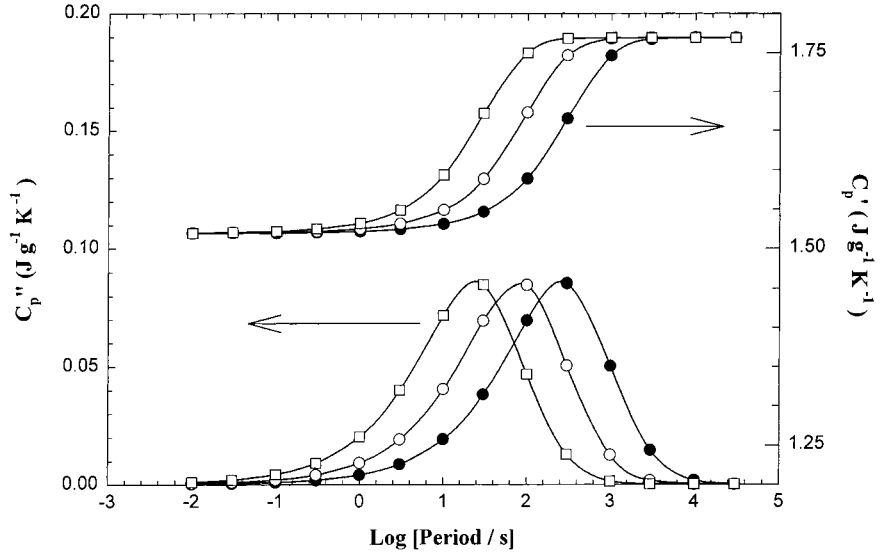

Fig. 3. Dynamic heat capacity quantities C_p' and C_p'' vs. logarithm of modulation period for polystyrene calculated from the Tool–Narayanaswamy equation of structural recovery. Temperature: (□) 95°C; (○) 93°C; (●) 91°C.

sing, and average (or total) heat flows are shown in units of heat capacity J/g K; the heat flow can be obtained by multiplying the heat capacities by the underlying heating rate. Both the reversing and non-reversing curves are smoothed. The simulated DSC response using the same experimental conditions but no modulation is also shown as a dotted line. Comparing the TMDSC average heat capacity with the analogous DSC result demonstrates that the modulation did not significantly distort the material response for a heating rate of 1°C/min.

For the case presented in Fig. 4, the material shows an enthalpic overshoot of moderate size in the vicinity of the glass temperature. From the reversing heat

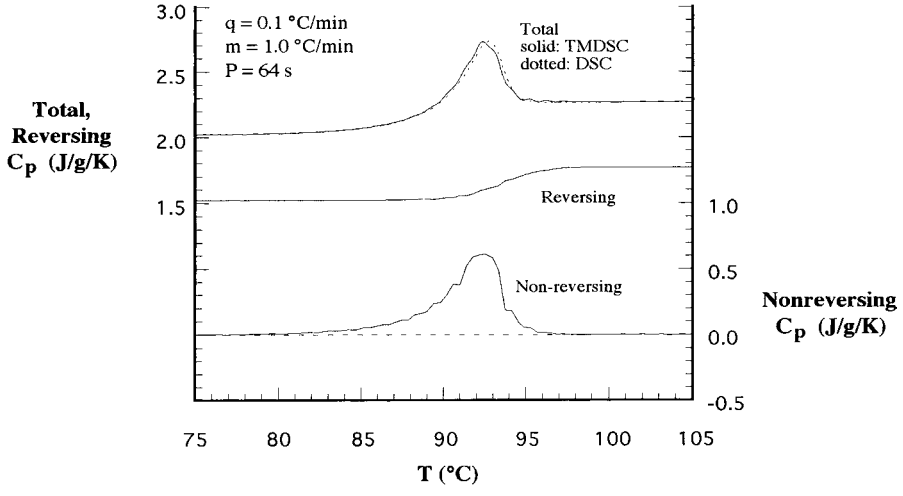

Fig. 4. Total, reversing, and non-reversing heat flow, in heat capacity units, for simulated polystyrene data for an enthalpy overshoot. The total heat flow is offset by 0.5 J/g K for clarity. The results of the analogous unmodulated DSC simulation are also shown.

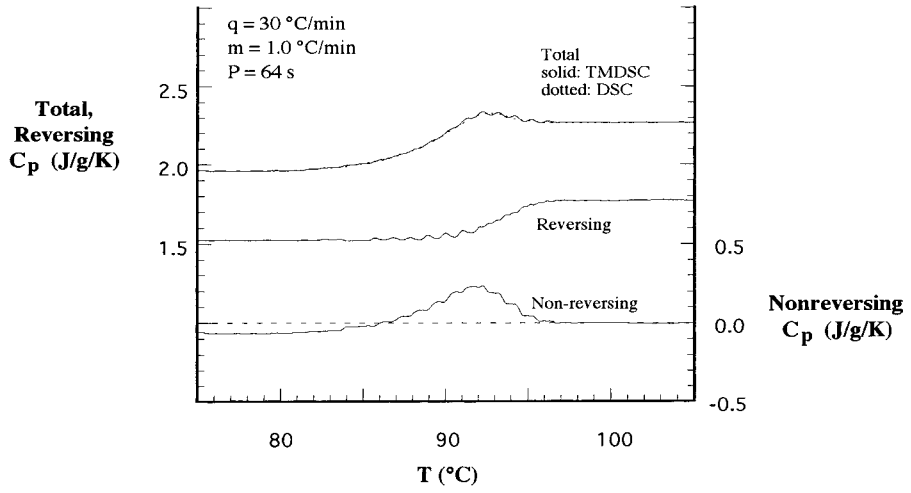

Fig. 5. Total, reversing, and non-reversing heat flow, in heat capacity units, for simulated polystyrene data for an enthalpy undershoot. The total heat flow is offset by 0.5 J/g K for clarity. The results of the analogous unmodulated DSC simulation are also shown.

capacity in Fig. 4, a value of 93.5°C is obtained for $T_{g,rev}$ from the midpoint of the step change. This is similar to the value of T_g of 93.4°C that we expect based on our isothermal linear simulations. From the non-reversing heat capacity, we obtain the enthalpy change due to relaxation during cooling, ΔH_{non}, of 2.7 J/g. The value of ΔH_a expected was 2.8 J/g. The agreement between the values of T_g and $T_{g,rev}$ and between ΔH_a and ΔH_{non} indicate that for this case the assumptions in the TMDSC data analysis described previously lead to no significant errors.

Fig. 5 shows the second case in which a small enthalpy undershoot below the glass temperature is present. In this case, the simulated experiment involved cooling at a higher rate, 30°C/min, followed by heating at an underlying rate of 1.0°C/min. The modulation period is 64 s. Again, the average, reversing, and non-reversing heat capacities are shown along with the heat capacity from a simulated DSC experiment using the same experimental conditions. Similar to the data for an underlying heating rate of 1°C/min, the average heat capacity from TMDSC for a heating rate of 0.1°C/min is undistorted compared to the DSC response.

From the reversing heat capacity in Fig. 5, the value of $T_{g,rev}$ is 93.1°C compared to the expected value of 93.4°C. The area under the non-reversing heat flow, ΔH_{non} is 1.4 J/g, whereas the expected area is 0.5 J/g. The difference is attributed to the fact that the enthalpy undershoot results in a broad exothermic relaxation peak at temperatures below T_g; in Fig. 5, this is observed as the area below the dashed line at 0.0 J/g K. Using a sloping baseline, thus, overestimates the non-reversing heat flow because it neglects the broad exotherm which should be subtracted from the total area. In the simulation, we can obtain results much closer to the correct answer (0.3 J/g) by integrating from zero over the entire temperature range rather than using a sloping baseline. In a real experiment, however, the value of the non-reversing heat flow is not zero in the absence of kinetic events; rather its value depends on the heat capacity calibration and the stability and curvature of the baseline. Consequently, it is not possible in a real experiment to obtain the correct value for ΔH_a for this case where there is a small enthalpy undershoot.

The situation is worse for larger undershoots as we show a little later. Fortunately, however, there are characteristic features present in the TMDSC scans that indicate that an undershoot is present and that the value of ΔH_{non} may have substantial error. These features include (1) the need to use a sigmoidal baseline in order to have the baseline tangent to the non-reversing heat flow on either side of the peak, and (2) a difference in the apparent temperature dependence of ΔC_p measured from the total and reversing heat flows. For example, for the case shown in Fig. 5, ΔC_p determined from the reversing heat flow is constant

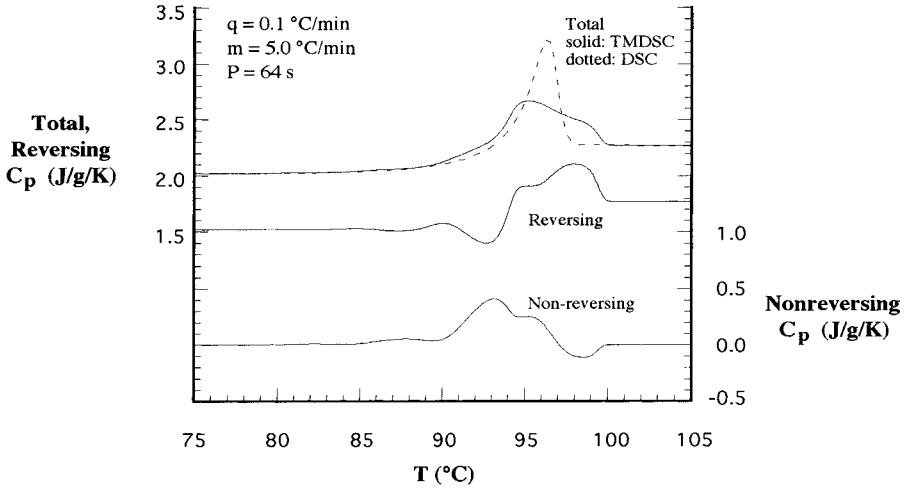

Fig. 6. Total, reversing, and non-reversing heat flow, in heat capacity units, for simulated polystyrene TMDSC data for a case with less than four cycles through the transition. The total heat flow is offset by 0.5 J/g K for clarity. The results of the analogous unmodulated DSC simulation are also shown.

and equal to the correct value of 0.25 J/g K. ΔC_p from the total heat flow is somewhat ambiguous, but if the tangent is taken far from T_g in the region where the glass heat capacity appears to be constant, a value of 0.32 J/g K is obtained for ΔC_p at T_g, which is significantly higher than the correct value of 0.25 J/g K.

The third case we examine is that in which the heating rate is high relative to the modulation period. Fig. 6 shows the results for simulated TMDSC data for polystyrene cooled at a slow rate, 0.1°C/min, but now having an underlying heating rate of 5°C/min. The period is 64 s. The average, reversing, and non-reversing heat capacities are shown, along with the simulated DSC response using the same experimental conditions. An enthalpy overshoot is observed as expected since the cooling rate is significantly lower than the heating rate. However, unlike the data shown in Figs. 4 and 5, calculated for an underlying heating rate of 1°C/min, the average heat capacity is substantially distorted compared to the DSC response. This might be expected because the glass transition is approximately 10°C wide and for a modulation period of 64 s and a heating rate of 5°C/min, less than two modulation cycles occur in the transition region.

Even though the heat flow is distorted by the modulation, we still obtain a value of 93.9°C for the midpoint of the reversing heat flow compared to the expected value of 93.4°C. On the other hand, the value of the area under the non-reversing heat flow, ΔH_{non}, is 1.8 J/g compared to the expected value of 2.8 J/g. Simply changing the period to 16 s resolves this problem: $T_{g,rev}$ is 96.6°C comparable to the expected value of 95.7°C, and ΔH_{non} is 3.4 J/g and is equal to the expected value.

5. Discussion

In the above, we described three cases that are encountered in TMDSC experiments: that of an enthalpy overshoot, an enthalpy undershoot, and a case in which the heating rate distorts the heat flow. In all cases discussed, the value of T_g obtained from the reversing heat flow was comparable to that expected from the linear simulations. The results from all of our simulations are shown in Fig. 7 in a plot of T_g and $T_{g,rev}$ vs. modulation period. In the figure, we differentiate the simulations in which there were more than four cycles through the transition and those in which there were not. The expected trend of a decreasing glass transition temperature with increasing period (decreasing frequency) is observed for both the linear isothermal calculations and for the TMDSC simulated data. $T_{g,rev}$ is within 1.0°C of T_g for experimental conditions where there are at least four cycles through the transition. Larger errors can be observed when

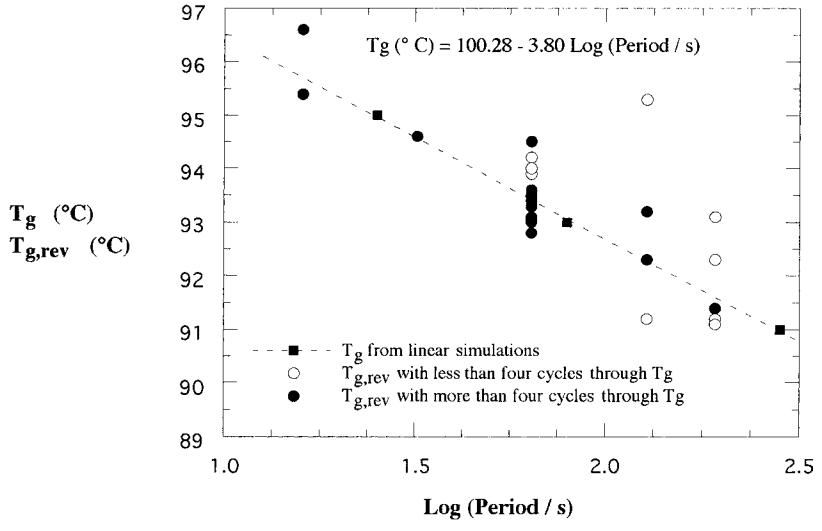

Fig. 7. T_g and $T_{g,rev}$ as a function of the modulation period from linear simulations and TMDSC simulations. The linear simulations give the expected frequency dependence of the measured T_g.

there are not adequate cycles through the transition as shown.

Errors of 1°C or less in the measurement of the glass transition temperature are not significant in many applications. More important than the fact that $T_{g,rev}$ approximates T_g is that since the reversing value does not have enthalpy overshoots or undershoots associated with it, it is actually more representative of the material than if a glass transition temperature were erroneously obtained from a scan that contained an enthalpy overshoot or undershoot. For example, if the peak temperature or the midpoint from the total heat capacity in Fig. 4 were used erroneously to calculate T_g, the value would be off by considerably more than 1°. For the case shown in Fig. 4, the value would be low. However, annealing peaks can occur up to 20 or 30°C above T_g giving erroneously high values of T_g. Thus, we suggest that TMDSC is a practical and useful tool for obtaining T_g. Our conclusions are consistent with the experimental work of Boller et al. [26]. These researchers reported that the glass transition temperature of polystyrene could be measured on heating in TMDSC and that it depended on the modulation period and only weakly on the thermal history or degree of aging of the sample.

In the three cases described in the current work, the error in the area of the non-reversing heat flow is insignificant for the enthalpy overshoot when adequate cycles through the glass transition are present and when there is no significant enthalpy undershoot. When an enthalpy undershoot is present, on the other hand, the magnitude of error depends on the ratio of the cooling rate to the heating rate (q/m) because that governs the magnitude of undershoot. However, examination of Eq. (11) shows that the absolute value of ΔH_a should only depend on the logarithm of the cooling rate and on the period in TMDSC. The cooling rate fixes T_{fo} and the period fixes T_g. The relationship between ΔH_a and $\log q$ for data simulated using a period of 64 s are shown in Fig. 8 along with the expected value based on Eq. (11). For low q where enthalpy overshoots occur, the values of ΔH_a are nearly the same as the theoretical values; above a cooling rate of approximately 10°C/min, the error progressively increases as the degree of undershoot increases.

The trend of increasing error in ΔH_a with the ratio of the cooling to heating rates (q/m) is shown more clearly as a function of the q/m in Fig. 9 for all the simulated data. Also shown in the figure is the error range for ΔH_a obtained from repeat experiments in conventional DSC using two sequential heating scans. The typical error in conventional DSC is on the order of 0.1 J/g (0.05 cal/g); see for example [27] for the scatter in ΔH_a obtained in conventional DSC. For data in which there are less than four cycles in the transition

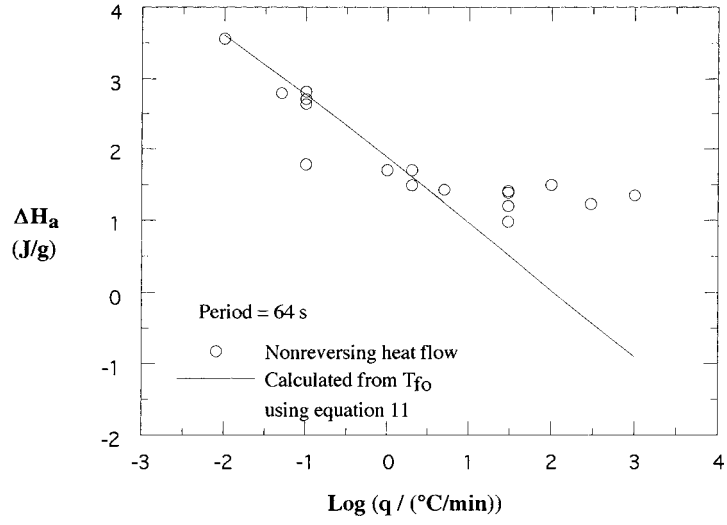

Fig. 8. Enthalpy of aging as a function of cooling rate q. The data points were obtained from the non-reversing heat flow for simulated data having a modulation period of 64 s. The line shows the expected trend based on Eq. (11) using T_{fo} from the simulated data and the expected value of T_g.

the error is generally substantially greater than this value. At low q/m, errors in ΔH_a from TMDSC are relatively small but the scatter is greater than 0.1 J/g even when sufficient cycles are present through the transition. On the other hand, at high q/m, the error increases linearly with $\log(q/m)$.

It should be clear from examination of Fig. 5 and from the discussion, that the error at high q/m is due to the presence of an undershoot and hence ΔH_{non} is not correctly calculated. The origin of the error at low q/m, although not as large, is also of interest. This error may in part be due to ringing in the first harmonic of the

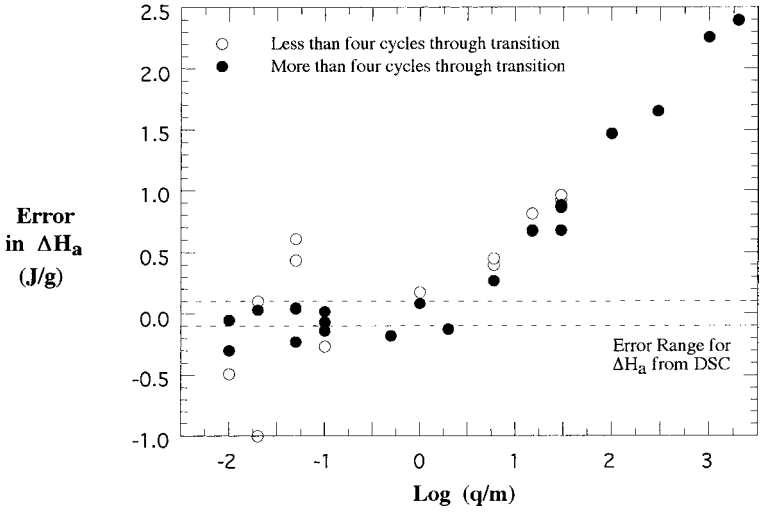

Fig. 9. Error in non-reversing heat flow as a function of the logarithm of the ratio of the cooling and heating rates. The typical error obtained in conventional DSC using two sequential scans is ±0.1 J/g.

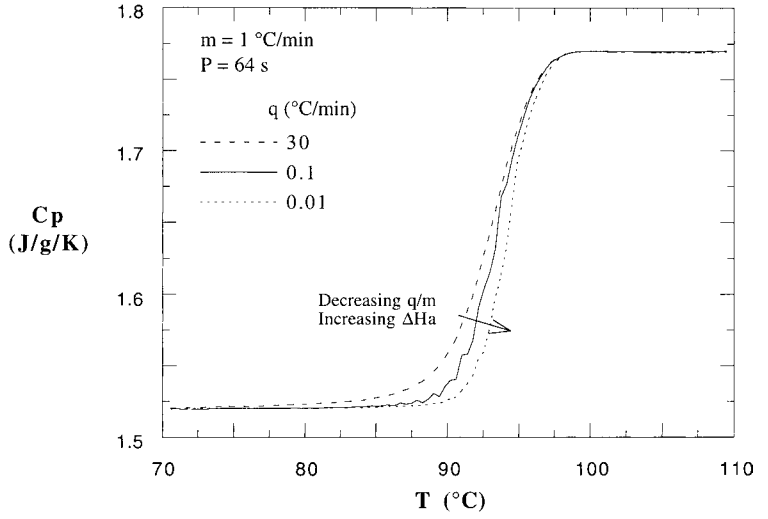

Fig. 10. Systematic change in reversing heat flow as a function of the magnitude of the enthalpic overshoot.

Fourier transform which has been attributed by Wunderlich et al. to a Doppler-like effect due to the temperature ramp [28]. The primary source of error, however, arises from the erroneous assumption that the reversing heat flow can be represented by the first harmonic; in other words, the step change at the glass transition contributes only to the first harmonic in the heat flow and that the structural recovery leading to the annealing peak does not. If this assumption were valid, we would expect to obtain the same reversing heat flow for a given period independent of the magnitude of the enthalpy recovery peak. In Fig. 10, we show that the reversing heat flow depends in a systematic way on the value of q/m (or the magnitude of ΔH_a) with a shift in the step change in T_g to higher temperatures as q/m decreases. A similar trend was observed but not discussed by Boller et al. [26]. Also consistent with our results, Wunderlich et al. have noted in subsequent publications that there is a contribution from the second harmonic to the reversing heat flow which results in an error in the reversing heat flow [28,29].

We showed in our earlier work [11] that the degree of non-linearity in the TMDSC data was related to the magnitude of the excess enthalpy annealing peak while comparing simulated data for the same scan rate and different cooling rates and indicated that caution needed to be used when interpreting TMDSC data due to the non-linearity. Here we have quantified the errors and have shown that the $T_{g,rev}$ is within 1.0°C of the expected value for experimental conditions where there are more than four cycles through the transition. On the other hand, the error in ΔH_a arises from three sources: enthalpy undershoots, contributions of structural recovery to the first harmonic, and interactions between the dynamic measurements made during a temperature ramp when the a low frequency probe is coupled with a high scanning rate.

6. Conclusions

Structural recovery in polymeric glass formers gives rise to the rich behavior observed during heating through the glass transition. For example, heating after slow cooling leads to an annealing peak or enthalpy overshoot in DSC heating experiments. Similarly, enthalpy undershoots are observed when the material relaxes during heating after fast cooling. One common model for describing these phenomena is the TNM equation. Here we used the TNM equation to simulate typical TMDSC data for various cooling and heating rates and modulation periods. We analyze the data using a fast Fourier transform to obtain the average, reversing, and non-reversing heat flows. The non-reversing heat flow is used to compute the fictive temperature of the aged glass and the enthalpy of aging and these are compared to the values expected from the input simulated data. The errors associated

with the data analysis were thus quantified and were used to test the primary assumption underlying analysis of TMDSC data — that the kinetics associated with a heat flow event show up only in the non-linear component of the heat flow signal and that the underlying change in the heat capacity is reflected only in the linear portion, i.e., the first harmonic of the heat flow signal. The assumption was found to break down in the glass transition region when there are enthalpy overshoots or enthalpy undershoots. In all cases, however, the glass temperature approximated from the reversing heat flow is a function of the modulation period and is independent of the cooling and heating rates giving a value for the glass temperature to within 1°C for a given period as long as four cycles are present in the transition region.

Although different instrument manufacturers use different methods of controlling or measuring the heat flow or different waveforms in their temperature modulation,..., we suggest that our analysis relevant to all TMDSC type instruments whenever the data analysis assumes that the reversing heat flow can be represented by the first harmonic in the heat flow response.

Acknowledgements

Partial support for this work from American Chemical Society Petroleum Research Fund, Grant No. 32555 AC7, is gratefully acknowledged.

References

[1] Modulated DSCTM Compendium: Basic Theory and Experimental Considerations, TA Instruments literature.
[2] M. Reading, TRIP 1 (1993) 248.
[3] S.E.B. Petrie, J. Polym. Sci., Part A-2, 10 (1972) 1255.
[4] B. Wunderlich, Y. Jin, A. Boller, Thermochim. Acta 238 (1994) 277.
[5] C.R. Snyder, F.I. Mopsik, J. Chem. Phys. 110 (2) (1999) 1106.
[6] J.E.K. Schawe, Thermochim. Acta 271 (1996) 127.
[7] N.O. Birge, S.R. Nagel, Phys. Rev. Lett. 54 (25) (1985) 2674.
[8] N.O. Birge, S.R. Nagel, Rev. Sci. Instrum. 58 (8) (1987) 1464.
[9] J.M. Hutchinson, S. Montserrat, Thermochim. Acta 304 (1997) 257.
[10] O.S. Narayanasamy, J. Am. Ceram. Soc. 54 (1971) 491.
[11] C.T. Moynihan, P.B. Macedo, C.J. Montrose, P.K. Gupta, M.A. DeBolt, J.F. Dill, B.E. Dom, P.W. Drake, A.J. Easteal, P.B. Elterman, R.P. Moeller, H. Sasabe, J.A. Wilder, Ann. N.Y. Acad. Sci. 279 (1976) 15.
[12] S.L. Simon, G.B. McKenna, Thermochim. Acta 307 (1997) 1.
[13] A.Q. Tool, J. Am. Ceram. Soc. 29 (1946) 240.
[14] I.M. Hodge, J. Non-Cryst. Solids 169 (1994) 211.
[15] J.M. O'Reilly, CRC Crit. Rev. Solid State Mater. Sci. 13 (1987) 259.
[16] R.W. Rendell, J.J. Aklonis, K.L. Ngai, G.R. Fong, Macromolecules 20 (1987) 1070.
[17] G.B. McKenna, in: C. Booth, C. Price (Eds.), Comprehensive Polymer Science, Vol. 12, Polymer Properties, Pergamon Press, Oxford, 1989, p. 311.
[18] G.B. McKenna, S.L. Simon, Time dependent volume and enthalpy responses in polymers, in: R.A. Schapery (Ed.), Time Dependent and Non-linear Effects in Polymers and Composites, American Society of Testing and Materials, Special Technical Publication, STP 1357, 2000, pp. 18–46.
[19] R. Kohlrausch, Prog. Ann. Phys. 91 (1854) 198.
[20] G. Williams, D.C. Watts, Trans. Faraday Soc. 66 (1970) 80.
[21] T.G. Fax, P.J. Flory, J. Appl. Phys. 21 (1950) 581.
[22] U. Gaur, B.B. Wunderlich, B. Wunderlich, J. Phys. Chem. Ref. Data 12 (1983) 29.
[23] S.L. Simon, D.J. Plazek, T. Holden, unpublished data.
[24] MATLAB, Version 5, Mathworks, Inc.
[25] S.L. Simon, G.B. McKenna, J. Chem. Phys. 107 (20) (1997) 8678.
[26] A. Boller, C. Schick, B. Wunderlich, Thermochim. Acta 266 (1995) 97.
[27] I. Echeverria, P.-C. Su, S.L. Simon, D.J. Plazek, J. Polym. Sci. Part B 33 (1995) 2457.
[28] B. Wunderlich, A. Boller, I. Okazaki, K. Ishikiriyama, Thermochim. Acta 304/305 (1997) 125.
[29] B. Wunderlich, I. Okazaki, J. Thermal Anal. 49 (1997) 57.